J Low Temp Phys (2008) 150: 267–275
DOI 10.1007/s10909-007-9545-0

Supersolidity and Disorder in Solid Helium 4

Frédéric Caupin · Satoshi Sasaki · Sébastien Balibar

Received: 27 July 2007 / Accepted: 28 September 2007 / Published online: 22 November 2007

Abstract Supersolidity is a rather controversial issue which has been revived recently by a number of torsional oscillator (ac-rotation) experiments with solid helium 4. One possibility would be that the ground state of helium 4 crystals contains a Bose-Einstein condensate of mobile vacancies. However, the supersolid signal was shown to depend on sample history. In addition, dc-flow experiments show that superfluid transport of mass does not occur in solid helium, except if it contains appropriate grain boundaries. As a consequence, we believe that supersolidity is not an intrinsic property of helium single crystals, but that it is due to quenched disorder. We report experiments on pressure relaxation in and light scattering from solid samples, that give additional evidence for the existence of disorder in helium crystals. We also describe our recent study of the wetting properties of grain boundaries.

Keywords Supersolids · Crystal growth · Disorder and porous media · Superfluid ^{4}He · Droplets, films, interfaces and wetting

PACS 67.80.Mg · 61.72.Mm · 68.08.Bc · 67.40.Hf · 67.40.-w · 67.90.+z

1 Introduction

Torsional oscillator (TO) experiments [1, 2] have revived the interest about solid helium 4 at low temperature. Below $T_c = 230\,\mathrm{mK}$, the resonant period of a TO filled with solid helium drops, showing that part of the solid mass decouples from the TO. This is similar to what is observed when cooling liquid helium 4 below 2.17 K, and

F. Caupin (✉) · S. Sasaki · S. Balibar
Laboratoire de Physique Statistique de l'Ecole Normale Supérieure, ENS-CNRS-Paris 6-Paris 7, 24, rue Lhomond, 75005 Paris, France
e-mail: caupin@lps.ens.fr

suggests that solid helium exhibits superfluid-like behavior. To describe this paradoxical state where crystalline order and superfluidity coexist, the word *supersolid* has been coined. The relative period shift of the TO is called the nonclassical rotational inertia fraction (NCRIF) and identified with the supersolid fraction.

Supersolidity was first proposed to originate from the Bose condensation of delocalized zero point vacancies in the crystal [3–6]. However, several experiments and theoretical results have shown that supersolidity was not (at least not only) an intrinsic property of perfect helium crystals. In Sect. 2, we briefly review the recent experimental work that puts forward the role of disorder. We then recall the work on DC flow of solid helium (Sect. 3), which triggered our interest for grain boundaries (GB). We then describe our recent results on the wetting properties of GBs [7] (Sect. 4), and finally discuss the implications for supersolidity (Sect. 5).

2 Evidence of the Role of Disorder

In TO experiments, the NCRIF saturates to a maximum value η_0 at low temperature. This maximum supersolid fraction varies between samples, and depends on each sample history. Annealing effects have been reported by different groups [8–10]. A sample is first grown at high temperature and constant volume with the blocked capillary method (BCM), and cooled down to measure η_0. The sample is then annealed close to melting, and cooled down again. All possible behaviors for η_0 have been reported: no change [10], increase by 10% [9], and reduction below the experimental uncertainty [8]. Recently, Clark et al. [11] have grown samples at low temperature and constant pressure, which is believed to produce crystals of higher quality than the BCM. They found lower values of η_0 than with the BCM. They also found annealing effects, but after several annealing cycles, η_0 seems to converge to a constant, non-zero value.

Conversely, η_0 can be increased by creating more disorder in a sample [12]. A solid grown by the BCM gave $\eta_0 = 6\%$ at $P = 41$ MPa (measured with a capacitive pressure gauge). It was then submitted to a short heat pulse, sufficient to melt it, but it recrystallized immediately because of the large surface-volume ratio of the TO. This created elastic strains in the solid, as revealed by the pressure increase to 51 MPa, and presumably a large disorder: η_0 now reached 20%.

This last experiment points out another difficulty in comparing data on different samples. They are usually reported at a given pressure. This pressure is measured either with a strain gauge on the TO wall, or with a capacitive gauge. But in fact, there is no reason that pressure should be homogeneous in a solid. Figure 1 illustrates this point. We grew a crystal with the BCM and cooled down to a given temperature T. Pressure was measured with a capacitive gauge connected to the cell by a capillary (0.6 mm inner diameter, 50 mm long). The solid was then melted, until the liquid-solid (LS) interface was visible in the main cell, so that the pressure there was the melting pressure $P_m(T)$. The pressure measured by the gauge slowly relaxed, but did not reach $P_m(T)$, which shows that elastic stress gradients remain, presumably concentrated in the capillary. In the case of the hcp crystal, the pressure excess was observed to last at least 10 hours, and we checked that the pressure eventually reached P_m after complete melting (lower right corner of Fig. 1).

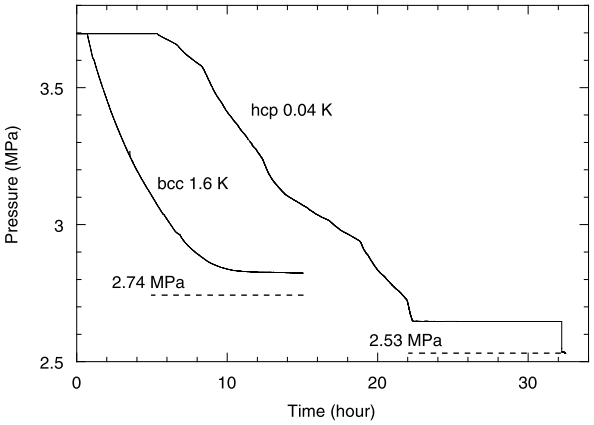

Fig. 1 Pressure relaxation at constant temperature for two different crystals grown with the BCM (see labels). The time origin is the instant when the LS interface was brought into the cell. The constant pressure at early times is due to saturation of the pressure gauge. The gauge reading relaxed, but to a value higher than the equilibrium melting pressure P_m corresponding to each experimental temperature (shown as *dashed lines*). We checked that it eventually reached P_m when the solid was totally melted (end of the trace for the hcp crystal)

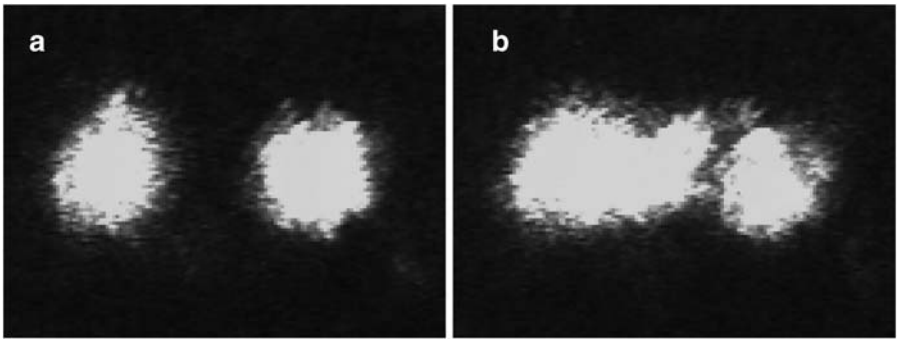

Fig. 2 Scattered light from a cell filled with liquid (**a**). The *two spots* correspond to the light scattered from the rear and front windows. They are spatially separated because we use an oblique incidence of the laser beam. After filling the cell with solid grown by fast injection at low temperature, additional scattering was observed (**b**), revealing the presence of inhomogeneities in density (for instance liquid droplets) with sizes comparable to the wavelength of light (600 nm)

In our recent experiments reported in Sect. 4, the solid was grown by fast injection at low temperature in a thin experimental cell. This is also expected to result in a highly disordered solid. By imaging the solid sample and focusing on one of the window, we can actually see a rough structure (not shown) [13]. To check the solid quality, we performed a simple light scattering experiment. We shine a laser beam through the cell, and look at the scattered light with an ordinary CCD camera. We choose an oblique incidence in order to separate the scattering from each window, as shown in Fig. 2a with the cell filled with liquid. After filling the cell with solid by fast injection, additional scattering was detected, coming from the center of the

cell (Fig. 2b). This shows that this fast injected solid contained regions of different density (for instance liquid droplets), otherwise there would be no local variation of the refractive index. The size of these regions is presumably comparable to the wavelength of light (600 nm) since no macroscopic grains could be seen.

Before describing our further studies on these samples (Sect. 4), we recall the work on DC flow, where GBs were shown to play a role.

3 DC Flow Experiments

Superfluid helium has the ability to flow in narrow channels without dissipation, provided that the flow velocity v is less than a critical velocity v_c. One would expect a supersolid to behave in a similar way. Day and Beamish [14] looked for flow of solid helium 4 through an array of 36000 glass capillaries (each 25 μm inner diameter, 3 mm long), in response to an applied pressure jump of 10 kPa. At 1.95 K near melting, flow occurs and the pressure relaxes within half an hour. In contrast, at low temperature (35 and 500 mK), no flow was detected over a period of about 20 hours. From the sensitivity of the capacitive pressure gauge and the total open area of the capillaries (0.18 cm^2), this sets an upper bound of $1.2\,10^{-14}\,m\,s^{-1}$ on v. If the supersolid fraction is 1% [1, 2], this corresponds to $v_c < 1.2\,10^{-12}\,m\,s^{-1}$, 7 orders of magnitude smaller than v_c obtained from TO experiments [1, 2].

We then looked for flow in a more open geometry. We used an inverted test tube (10 mm diameter) in an experiment *à la* Torricelli: the top of the tube is closed, the bottom dips in solid helium but is kept 10 mm above the bottom of the cell, and we manage to have a level difference h between the LS interface inside and outside the tube [15, 16]. We observed that, in good quality crystals at 50 mK, h remained constant within 50 μm over 4 hours, corresponding to v at least 300 times less than what one would expect from the TO results. However, in two lower quality crystals with grain boundaries (as revealed by the presence of cusps at the LS interface), flow did occur at 50 mK, with a different but constant velocity in each crystal, which is characteristic of superflow. If one assumes that a few atomic layers thick GBs are superfluid, this would correspond to v_c of a few $m\,s^{-1}$. A similar value was measured in liquid films of atomic thickness [17]. Finally, in a third crystal with many cusps, we observed a similar superflow at 1.13 K, suggesting that a GB could be thick enough to exhibit a high T_c. We decided to investigate more closely the behavior of a single GB, as explained in Sect. 4.

4 Wetting Properties of Grain Boundaries

We grow the solid by fast injection at low temperature, as described in Sect. 2. When the pressure is released, the solid in the cell is brought close to melting, and a cloud of small grains appear, which further ripen into larger grains as liquid enters at the top of the cell, leading to a foam-like solid. As helium is removed from the cell, ripening proceeds, until a few grains remain. By slowly injecting and removing helium, we are in most cases able to select two grains, and to drive the GB into a vertical plane

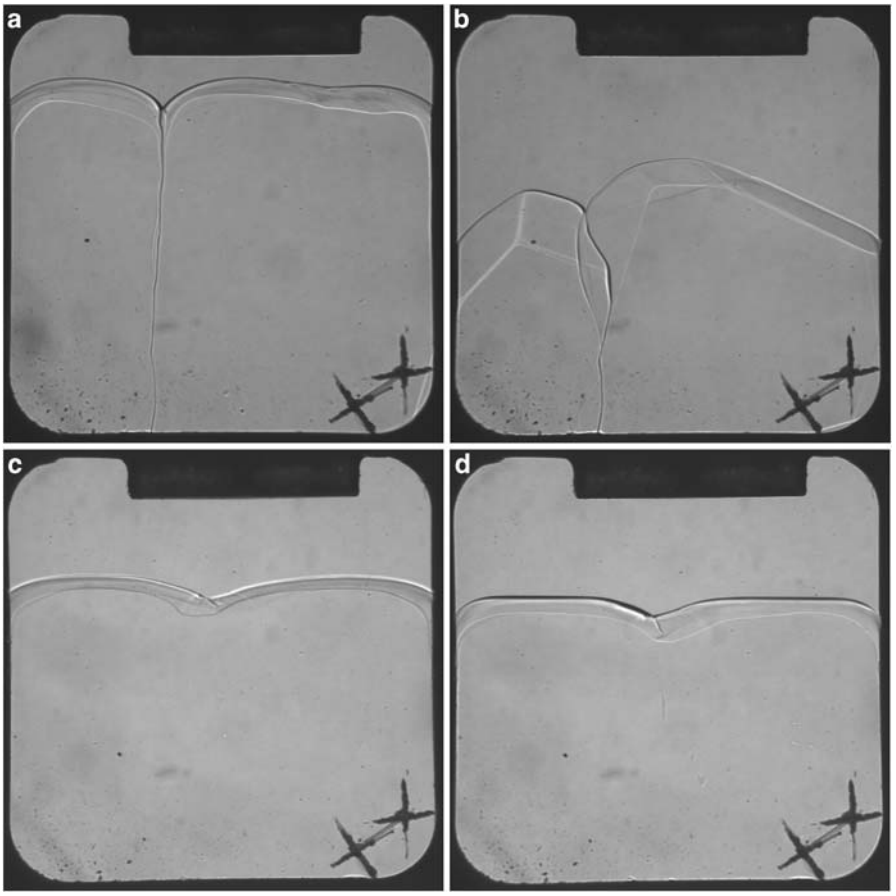

Fig. 3 Two couples of images showing equilibrium shapes (**a**, **c**) together with growth shapes which reveal the crystal orientation (**b**, **d**). When the two crystal grains have a large difference in orientation (**a**, **b**), their boundary ends as a deep groove at the LS interface. The contact lines of the GB with the windows are in fact liquid channels (*vertical lines* in (**a**, **b**)). Crystals with similar orientations can be obtained by direct growth (**c**, **d**). In this case, the groove is shallow with no liquid channels on the windows. Two crosses carved on the windows (*lower right corners*) help adjusting the focusing. The cell dimensions are 11 mm × 11 mm × 3 mm

nearly perpendicular to the windows. An example is given in Fig. 3a. The orientation of each crystal can be deduced from growth shapes (Fig. 3b).

The GB emerging at the LS interface makes a groove whose dihedral angle 2θ we studied. Care was taken to look along the groove axis. The LS interface profiles on each side were fitted near the GB with a one dimensional Laplace law to obtain 2θ. For three different samples, we found the values $\theta = 11 \pm 3$, 16 ± 3, and $14.5 \pm 4°$. These non-zero values show that the GB is not wetted by the liquid phase (absence of pre-melting), in agreement with recent simulations [18] which estimate that the thickness of the GB remains microscopic (around 3 atomic layers). This gives an information about the GB surface energy σ_{GB}: if, for simplicity, one neglects the

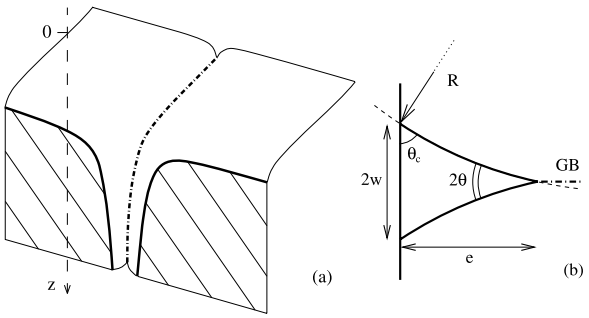

Fig. 4 (**a**) Three dimensional view of the contact between a grain boundary (*dash-dotted line*) and a wall. The hatched area shows the contact of the wall with the solid. (**b**) Horizontal cross section of the liquid channel near the wall

anisotropy of the LS surface tension σ_{LS}, mechanical equilibrium requires

$$\sigma_{GB} = 2\sigma_{LS} \cos\theta. \tag{1}$$

We can check the consistency of the values found for θ using the relation between the depth Δz of the groove and the known value of σ_{LS} [19]:

$$(\rho_S - \rho_L) g (\Delta z)^2 = 2\sigma_{LS}(1 - \sin\theta) \tag{2}$$

with ρ_L (resp. ρ_S) the mass per unit volume of the liquid (resp. the solid), and g the gravity. Note that, in materials science, a similar relation is widely used to measure σ_{LS} [20, 21], where the effect of gravity is replaced by a thermal gradient.

Next, Fig. 3a shows that the contact between the GB and the glass windows is a liquid channel. This can be understood with a simple model. If we neglect the anisotropy of σ_{LS} and elastic effects, the force balance on the contact line between the liquid and the GB requires this GB to be a vertical plane perpendicular to the wall, and the liquid channel to be symmetric with respect to this plane (see Fig. 4). The LS interface makes a contact angle θ_c with the glass wall. We have $\cos\theta_c = (\sigma_{SW} - \sigma_{LW})/\sigma_{LS}$, where σ_{SW} and σ_{LW} are the solid-wall and liquid-wall surface tensions, respectively. We were able to check the previous estimate of θ_c [19] by imaging the contact with the copper walls and the glass plate at the top of the cell. We confirm that $\theta_c \simeq 45°$, but we noticed a large scatter due to hysteresis and pinning effects.

Hydrostatic equilibrium in the liquid implies that the liquid pressure is $P_L(z) = P_{eq} + \rho_L g z$, where z is the depth measured from the nearly flat top of the grains. The equality of chemical potentials at the LS interface requires the pressure in the solid to be $P_S(z) = P_{eq} + \rho_S g z$. Laplace equation gives the radius of curvature R of the LS interface. For $z/l_c > 1.7$, where l_c is the capillary length $\sqrt{\sigma_{LS}/[(\rho_S - \rho_L)\, g]} \approx 1\,\text{mm}$, the curvature in the horizontal plane dominates, and $R = \sigma_{LS}/[P_S(z) - P_L(z)] = {l_c}^2/z$ [13]. Figure 4b shows a horizontal cross section of the channel, defining its thickness e and width $2w$. Trigonometric relations lead to:

$$e(z) = \frac{{l_c}^2}{z}(\cos\theta_c - \sin\theta), \tag{3}$$

$$w(z) = \frac{{l_c}^2}{z}(\cos\theta - \sin\theta_c). \tag{4}$$

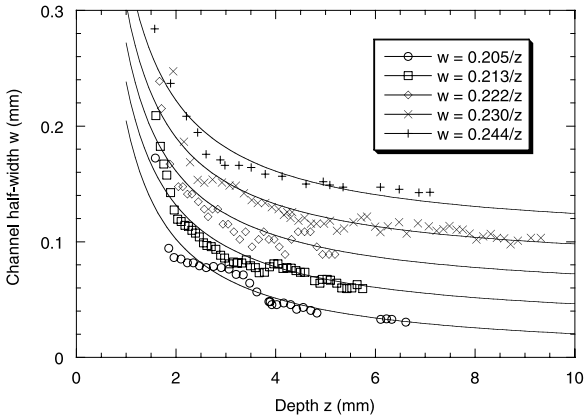

Fig. 5 The half-width w as a function of depth z for 5 different samples. Good agreement with (4) is found. Each data set has been shifted upward starting from the lowest one, in increments of 0.025 mm to avoid overlaps

The liquid channel exists if and only if $\theta + \theta_c < \pi/2$, a condition which was fulfilled in all samples we made by fast injection. On the other hand, we could make two grains with similar orientation by nucleation in the cell in response to a pressure pulse made by closing a valve on the fill line (Figs. 3c and 3d): they showed a shallower groove with larger θ, and no liquid channel, in agreement with the above condition.

For crystals showing channels, we measured the half-width w as a function of depth z by enlarging pictures such as Fig. 3a. Figure 5 shows five different fits with a relation $w = A/z$ of the five different data sets. We found A between 0.20 and 0.24 mm^2, which is consistent with (4). The channel width vanishes rapidly as P increases: $2w$ reaches 1 nm (the typical thickness of a GB [18]) at 0.94 MPa above P_{eq} [13]. Note that elastic effects could stabilize liquid channels at high pressure. We have also observed that the channels can be pinned to wall defects which locally favor the presence of the liquid phase.

The present results lead us to reconsider the interpretation of earlier experiments by Franck et al. [22, 23]. They studied films about 50 μm thick with a Schlieren method, at high temperature and above 50 MPa. For the fcc phase, a polygonal, foam-like structure was observed; upon heating, the vertices of the foam widened into a curved triangular shape, before melting occurred at the GBs, the grains of the crystal becoming separated. Measurement of the dihedral angle 2θ at a GB was difficult and gave $0° \leq 2\theta \leq 30°$. In contrast, the hcp phase exhibited banded structures, with no GB melting, which suggested partial wetting of the GBs, although 2θ could not be measured [23]. Because of the observations made for the fcc phase, this experiment is cited by Dash et al. as an evidence for near complete wetting [24] or even premelting [25] of the GBs. However, the films studied by Franck et al. were thin, with one side in contact with a glass window, and the other with the liquid. In our opinion, the above described liquid channels play a role in the structure of their thin films. We have shown that the channel width depends on the departure from P_{eq}; this would explain why the vertices of the foam widen upon heating, until the grains detach. It also explains why the contrast is lost when the temperature is lowered 50–100 mK below T_m [23]: it is not due to the disappearance of the GBs, because the contrast is recovered upon heating; we rather think that the channels shrink to sub-micrometer dimensions upon cooling, and widen again upon heating.

5 Discussion

Our findings about the wetting properties of GBs question the interpretation of our DC flow experiments (Sect. 3): the flow in the test tube requires a GB, but it could take place either along the GB, or along the two liquid channels it makes on the tube walls according to Sect. 4. In the latter case, taking 870 μm^2 for the cross section area of a channel at a depth $z = 10\,mm$ below the free LS interface [13], we find a critical velocity $v_c \simeq 3\,mm\,s^{-1}$ along the channel. This is a reasonable value for this channel size [26]. If mass was really transported along these channels, it would explain why relaxation took place at least up to 1.1 K while GBs are predicted to become superfluid only around 0.5 K [18]. Measurements in different cell geometries are required in order to decide which mechanism is relevant. It would also be interesting to investigate the temperature dependence.

A coherent picture to explain all the experimental findings is still lacking. However, the annealing or quenching experiments in TO studies emphasize the role of disorder. Our observations show how GB can be involved. There are other possibilities. The core of a screw dislocation is predicted to be superfluid [27] below 1 K. A network of such cores could explain the superfluid response in TO experiments, at a lower T_c because of coherence properties of the network [27]. In addition, different AC and DC behaviors are expected. It is also likely that there exists glassy or liquid regions in quenched samples, since annealing such samples produces a large pressure drop [12, 28]. In our cell, samples grown at constant volume do not show any significant light scattering. Either the liquid or glassy regions are not present or their size is too small compared to the wavelength of light.

Acknowledgements We are grateful to N. Jamal, H.J. Maris, P. Nozières, and E. Rolley for helpful discussions. This work is supported by ANR grant 05-BLAN-0084-01.

References

1. E. Kim, M.H.W. Chan, Nature **427**, 225 (2004)
2. E. Kim, M.H.W. Chan, Science **305**, 1941 (2004)
3. A.F. Andreev, I.M. Lifshitz, Sov. Phys. JETP **29**, 1107 (1969)
4. G.V. Chester, Phys. Rev. A **2**, 256 (1970)
5. A.J. Leggett, Phys. Rev. Lett. **25**, 1543 (1970)
6. D.E. Galli, L. Reatto, Phys. Rev. Lett. **96**, 165301 (2006)
7. S. Sasaki, F. Caupin, S. Balibar, Phys. Rev. Lett. **99**, 205302 (2007)
8. A.S. Rittner, J.D. Reppy, Phys. Rev. Lett. **97**, 165301 (2006)
9. A. Penzev, Y. Yasuta, M. Kubota, J. Low Temp. Phys. **148**, 677 (2007)
10. M. Kondo, S. Takada, Y. Shibayama, K. Shirahama, J. Low Temp. Phys. **148**, 695 (2007)
11. A.C. Clark, J.T. West, M.H.W. Chan, arXiv:0706.0906
12. A.S. Rittner, J.D. Reppy, Phys. Rev. Lett. **98**, 175302 (2007)
13. S. Sasaki, F. Caupin, S. Balibar, in preparation
14. J. Day, J. Beamish, Phys. Rev. Lett. **96**, 105304 (2006)
15. S. Sasaki, R. Ishiguro, F. Caupin, H.J. Maris, S. Balibar, Science **313**, 1098 (2006)
16. S. Sasaki, R. Ishiguro, F. Caupin, H.J. Maris, S. Balibar, J. Low Temp. Phys. **148**, 665 (2007)
17. K. Telschow, I. Rudnick, T.G. Wang, Phys. Rev. Lett. **32**, 1292 (1974)
18. L. Pollet, M. Boninsegni, A.B. Kuklov, N.V. Prokof'ev, B.V. Svistunov, M. Troyer, Phys. Rev. Lett. **98**, 135301 (2007)
19. S. Balibar, H. Alles, A.Y. Parshin, Rev. Mod. Phys. **77**, 317 (2005)

20. G.F. Bolling, W.A. Tiller, J. Appl. Phys. **31**, 1345 (1960)
21. U. Böyük, K. Keşlioğlu, N. Maraşh, J. Phys.: Condens. Matter **19**, 116202 (2007) and references therein
22. J.P. Franck, K.E. Kornelsen, J.R. Manuel, Phys. Rev. Lett. **50**, 1463 (1983)
23. J.P. Franck, J. Gleeson, K.E. Kornelsen, J.R. Manuel, K.A. McGreer, J. Low Temp. Phys. **58**, 153 (1985)
24. J.G. Dash, H.Y. Fu, J.S. Wettlaufer, Rep. Prog. Phys. **58**, 115 (1995) and references therein
25. J.G. Dash, J.S. Wettlaufer, Phys. Rev. Lett. **94**, 235301 (2005)
26. J. Wilks, *The Properties of Liquid and Solid Helium* (Clarendon Press, Oxford 1967), p. 390
27. M. Boninsegni, A.B. Kuklov, L. Pollet, N.V. Prokof'ev, B.V. Svistunov, M. Troyer, Phys. Rev. Lett. **99**, 035301 (2007)
28. V.N. Grigor'ev, V.A. Maidanov, V.Y. Rubanskii, S.P. Rubets, E.Y. Rudavskii, A.S. Rybalko, Y.V. Syrnikov, V.A. Tikhii, arXiv:cond-mat/0702133 (2007)